



Break-up of a set of liquid threads under influence of surface tension

A. Y. GUNAWAN, J. MOLENAAR¹ and A. A. F. VAN DE VEN¹

Departemen Matematika, Institut Teknologi Bandung, Indonesia; Email: a.y.gunawan@tue.nl

¹*Department of Mathematics and Computer Science, Eindhoven University of Technology, The Netherlands; Email: j.molenaar1@tue.nl*

Received 20 March 2003; accepted in revised form 17 December 2003

Abstract. In this paper it is shown how the long-standing problem of the break-up of a cylindrical interface due to surface tension can be generalized to an arbitrary number of interacting interfaces in an arbitrary configuration. A system of immersed threads starting with two types of configurations is studied, *i.e.*, a system of threads on a row and a system of threads at triangular vertices. From these cases, which are worked out in detail, it becomes clear how the stability of an arbitrary configuration can be determined. The (in)stability of the configuration is discussed in terms of the so-called disturbance growth rate. It turns out that the threads break up in specific phase patterns in which neighbouring threads are either in-phase or out-of-phase. For L threads, in principle 2^L phase patterns are possible. However, it is shown that the stability of the system directly follows from L so-called basic phase patterns. Special attention is paid to the special case of threads and fluid having equal viscosity. Then, the growth rate can be calculated analytically using Hankel transformations. An estimate for the growth rate in this case, which turns out to be quite sharp, is derived.

Key words: break-up, creeping flow, phase pattern, surface tension

1. Introduction

Nowadays, the demand for new synthetic materials is increasing and becoming more specific. New synthetic materials may be produced by blending different types of polymers. The material properties of a polymer blend are strongly related to its morphology determined by the blending process in an extruder. Therefore, the eventual material properties can be predicted only if a thorough understanding of this blending process is available. In the extruder, dry granules of two types of polymers are supplied into the hopper. Due to heating, by external heat sources and internal friction, the granules melt. In the melt, we distinguish between the dispersed phase and the continuous phase (or matrix phase). The polymer with the lowest volume fraction is called the dispersed phase. Subsequently, the blending takes place by the shear flow caused by the screw. Due to dominant shear stresses, long threads are formed. If the blend contains a large volume fraction of the threads, the interactions between the threads are of essential importance for the way they break up. Therefore, a mathematical model simulating the break-up behaviour may provide important insights for control of the production process such as for the spatial distribution of the droplets.

The study of the break-up of liquid threads has a distinguished history, starting with the work of Savart [1] in the early nineteenth century. He showed that the break-up of a jet of water always occurs, independently of the direction of gravity, the type of fluid, or the jet velocity and radius. Some years later, Plateau [2] discovered that the source of the break-up is

surface tension. The dynamical description of the problem, in terms of linear stability theory, was first given by Rayleigh [3]. He considered the stability of a long cylindrical column of an incompressible perfect (*i.e.*, inviscid) fluid under the action of capillary forces, neglecting the effect of the surrounding fluid. In his paper, Rayleigh developed the important concept of the *mode of maximum instability*. He showed that, from an initially small disturbance, a number of unstable waves may form on the jet surface; the wave that causes the jet to break up is the one with maximum instability, which is measured by the so-called *growth rate*, to be defined later on. The case of an incompressible, cylindrical column of viscous liquid has also been discussed by Rayleigh [4]. Assuming the viscosity to be dominating over the inertia and neglecting the effect of the surrounding fluid, he found that the maximum instability occurs when the wave length of the disturbance is very large in comparison with the radius of the initial cylinder. Following Rayleigh's approach, Tomotika [5, 6] generalized the analysis to include viscosity for both the fluid column and the surrounding fluid. He found that the instability of the jet is strongly influenced by the ratios of the viscosities and densities of jet and surrounding fluid, and of the Ohnesorge number, a dimensionless parameter representing the ratio of viscous and interfacial-tension forces. If the ratio of viscosities of the two fluids is neither zero nor infinite, the maximum instability always occurs at a definite wave length. A generalisation of Tomotika's stability analysis for several limiting cases such as low-viscosity liquid jet in a gas, gas jet in a low viscosity liquid, etc., was discussed by Meister and Scheele [7]. Mikami *et al.* [8] improved Tomotika's theory both theoretically and experimentally. The theoretical study of the break-up of a liquid thread is studied to some extent in [9, 10, 11, 12, 13, 14, 15]. A wide-ranging review of a large number of theoretical and experimental investigations of the break-up process of one thread is given by Eggers [16].

In [17], we extended the work of Tomotika by studying the dynamics of a set of two liquid threads immersed in a fluid. The system was modelled by the Stokes equations, which we solved by means of separation of variables in two systems of cylindrical coordinates, each one connected to one of the threads. The dependence on the azimuthal coordinates was expressed in terms of a Fourier expansion. We examined the influence of small initial disturbances of the threads based on both zero-order and first-order Fourier expansions. The results showed that the break-up behaviour of the threads is again determined by the growth rate q which in this case also depends on the distance b between the threads. The results also revealed that an extension from a zero to a first-order Fourier expansion leads to small quantitative corrections only. For the two-threads system, we found that the threads may break up either in-phase or out-of-phase. These findings were in agreement with the experiments reported in [18] and [19].

In the present work, we consider the dynamics of a number of L threads ($L > 2$) for two types of configurations. First, we consider the dynamics of a row of equally spaced immersed threads. Second, we determine the dynamics of the threads when they have a triangular configurations. The dynamics of the 3-threads system will be worked out by use of the zero-order Fourier expansion. This serves as a guide for the solution of the L -threads system with $L > 3$. Next, the instability of the L -threads system is determined. It turns out that the threads will disintegrate with neighbouring threads being either in-phase or out-of-phase. The instability problem leads to an L by L matrix differential equation. The behaviour of the system is determined by the eigenvalues of the matrix. We show how the eigenvectors are related to L so-called basic phase patterns. The break-up behaviour of the system as a whole can be expressed completely in terms of the behaviour of these basic patterns.

We also derive an analytical formula for the growth rate for the special case of threads and fluid having equal viscosities. In experiments, this corresponds to two immiscible fluids of equal viscosity. Stone and Brenner [20] provided a direct method to derive an explicit formula for the single-thread case. They used the idea of a ring force in which the normal stress jump at the interface arising from surface tension is represented by a delta function. The use of Hankel transforms then led to an explicit formula for the radial velocity and from that for the growth rate q . We extend this work by studying the non-axisymmetric breakup of L immersed threads. Thanks to the Toeplitz form of the matrix in our system of ODE's, we are able to present an analytical upper bound for the growth rate. Numerical evaluations show that this upper bound is quite close to the least upper bound.

The paper is organized as follows. In Section 2, the mathematical model for L immersed threads is derived both for threads on a row and for threads at triangle vertices. The solution is written in terms of a Fourier expansion. The zero-order mode solution is worked out and the solution for the unknown coefficients is presented. Based on this solution, the stability of the system is investigated. In Section 3, the stability of liquid threads immersed in a fluid is discussed, for the special case of threads and fluid having equal viscosities. For two threads an analytical formula for the growth rate is derived. For L threads ($L > 2$), an analytical upper bound for the growth rate is found. Results are given in Section 4 and conclusions in the last section.

2. Modelling L immersed threads

2.1. ROW CONFIGURATION

2.1.1. Mathematical model and solution methodology

Consider a sequence of L infinitely long parallel threads, equally spaced with distances b . All threads have viscosity η^d . They are surrounded by a fluid with viscosity η^c . The indices c and d refer to the continuous phase (surrounding fluid) and the dispersed phase (threads), respectively. We denote the ratio of the viscosities by

$$\mu = \frac{\eta^d}{\eta^c}. \quad (1)$$

For thread j ($j = 1, \dots, L$), a cylindrical coordinate system (r_j, ϕ_j, z_j) will be used with z measured along the thread. In Figure 1, the coordinates r_j and ϕ_j are indicated for a system with $L = 3$. In general, if thread J is taken as frame of reference, we have the relations ($j, J = 1, \dots, L$):

$$\begin{aligned} r_J \cos \phi_J &= (j - J)b + r_j \cos \phi_j, \\ r_J \sin \phi_J &= r_j \sin \phi_j, \\ z_J &= z_j. \end{aligned} \quad (2)$$

Let us consider a perturbation of threads, that is periodic in z with wave number k_j . Because the problem is not axisymmetric, the disturbance of thread j may also depend on ϕ_j . This dependence is represented by a Fourier expansion. The radius R_j of thread j is then written as

$$R_j(\phi_j, z, t) = a \left[1 + \sum_{m=0}^{\infty} \varepsilon_{j,m}(t) \cos m\phi_j \cos(k_j z - \alpha_j) \right]. \quad (3)$$

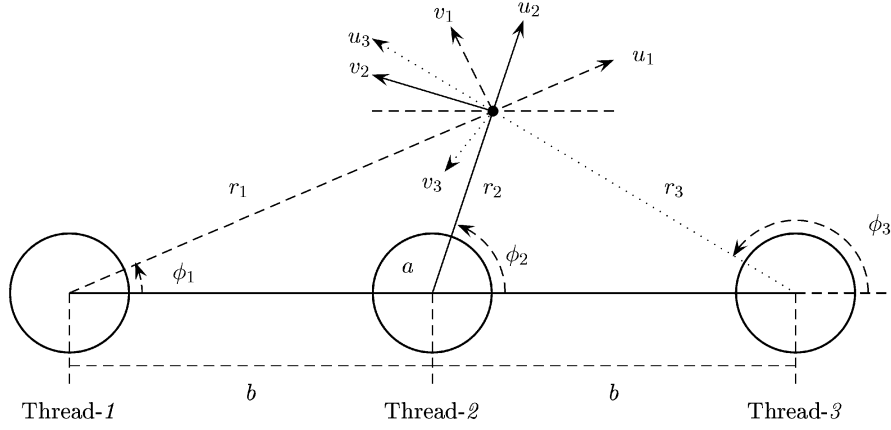


Figure 1. Cylindrical coordinate systems for $L = 3$.

Since the z -axes of all threads are parallel, we dropped the index j from the z -coordinates. Here, a is the initial radius of the threads, $\varepsilon_{j,m}$ is the time dependent amplitude of the m -th mode, and α_j is the phase of this mode. The $\varepsilon_{j,m}$ and α_j are unknown in advance.

The dynamics of the disintegrating threads under this perturbation is known if we calculate the velocity field \mathbf{v} . Since all movements are slow due to the high viscosity, we use the creeping flow approximation and assume \mathbf{v} to satisfy the Stokes equation. The fluids are incompressible, so the incompressibility condition holds. Thus, we model the system by:

$$\nabla \cdot \mathbf{v} = 0, \quad (4a)$$

$$\nabla p = \hat{\eta} \Delta \mathbf{v}. \quad (4b)$$

Here, p is the pressure and $\mathbf{v} = (u, v, w)$ are the velocities in radial, azimuthal and axial direction, respectively. Inside the threads we have $\hat{\eta} = \eta^d$ and outside the threads $\hat{\eta} = \eta^c$. In cylindrical coordinates, the Stokes equations in terms of the coordinate system attached to thread j read as

$$0 = \frac{1}{r_j} \frac{\partial}{\partial r_j} [r_j u_j] + \frac{1}{r_j} \frac{\partial v_j}{\partial \phi_j} + \frac{\partial w_j}{\partial z} \quad (5a)$$

$$\frac{\partial p_j}{\partial r_j} = \hat{\eta} \left[\frac{1}{r_j} \frac{\partial}{\partial r_j} \left[r_j \frac{\partial u_j}{\partial r_j} \right] + \frac{1}{r_j^2} \frac{\partial^2 u_j}{\partial \phi_j^2} + \frac{\partial^2 u_j}{\partial z^2} - \frac{2}{r_j^2} \frac{\partial v_j}{\partial \phi_j} - \frac{u_j}{r_j^2} \right] \quad (5b)$$

$$\frac{1}{r_j} \frac{\partial p_j}{\partial \phi_j} = \hat{\eta} \left[\frac{1}{r_j} \frac{\partial}{\partial r_j} \left[r_j \frac{\partial v_j}{\partial r_j} \right] + \frac{1}{r_j^2} \frac{\partial^2 v_j}{\partial \phi_j^2} + \frac{\partial^2 v_j}{\partial z^2} + \frac{2}{r_j^2} \frac{\partial u_j}{\partial \phi_j} - \frac{v_j}{r_j^2} \right] \quad (5c)$$

$$\frac{\partial p_j}{\partial z} = \hat{\eta} \left[\frac{1}{r_j} \frac{\partial}{\partial r_j} \left[r_j \frac{\partial w}{\partial r_j} \right] + \frac{1}{r_j^2} \frac{\partial^2 w_j}{\partial \phi_j^2} + \frac{\partial^2 w_j}{\partial z^2} \right]. \quad (5d)$$

The system is brought into dimensionless form if the following scalings are applied:

$$r_j = ar_j^*, \quad z = az^*, \quad b = ab^*, \quad R_j = aR_j^*, \quad \mathbf{v}_j = \frac{\sigma}{\eta^c} \mathbf{v}_j^*, \quad p_j = \frac{\sigma}{a} p_j^*, \quad \text{and } k_j a = k_j^*, \quad (6)$$

where σ is the surface tension. In the sequel we omit the asterisks, since confusion is not possible. Separating variables and expressing the dependence on ϕ in terms of Fourier modes, we propose as general expressions for the solution inside thread j :

$$p_j^d(r_j, \phi_j, z, t) = \sum_{m=0}^{\infty} p_{j,m}^d(r_j, t) \cos m\phi_j \cos(k_j z - \alpha_j), \quad (7a)$$

$$u_j^d(r_j, \phi_j, z, t) = \sum_{m=0}^{\infty} u_{j,m}^d(r_j, t) \cos m\phi_j \cos(k_j z - \alpha_j), \quad (7b)$$

$$v_j^d(r_j, \phi_j, z, t) = \sum_{m=1}^{\infty} v_{j,m}^d(r_j, t) \sin m\phi_j \cos(k_j z - \alpha_j), \quad (7c)$$

$$w_j^d(r_j, \phi_j, z, t) = \sum_{m=0}^{\infty} w_{j,m}^d(r_j, t) \cos m\phi_j \sin(k_j z - \alpha_j). \quad (7d)$$

The same holds for the continuous phase with the index d replaced by c . For example, the radial velocity of the continuous phase with respect to thread j for $j = 1, \dots, L$ is written as

$$u_j^c = \sum_{m=0}^{\infty} u_{j,m}^c(r_j, t) \cos m\phi_j \cos(k_j z - \alpha_j). \quad (8)$$

Substitution of (7) and (8) in (5) yields equations for the coefficients, $m \geq 0$,

$$0 = \frac{1}{r_j} \frac{\partial}{\partial r_j} [r_j u_{j,m}] + \frac{m}{r_j} v_{j,m} + k_j w_{j,m}, \quad (9a)$$

$$\frac{\partial p_{j,m}}{\partial r_j} = \hat{\eta} \left[\frac{1}{r_j} \frac{\partial}{\partial r_j} \left[r_j \frac{\partial u_{j,m}}{\partial r_j} \right] - \frac{m^2 + 1 + (k_j r_j)^2}{r_j^2} u_{j,m} - \frac{2m}{r_j^2} v_{j,m} \right], \quad (9b)$$

$$-\frac{m}{r_j} p_{j,m} = \hat{\eta} \left[\frac{1}{r_j} \frac{\partial}{\partial r_j} \left[r_j \frac{\partial v_{j,m}}{\partial r_j} \right] - \frac{m^2 + 1 + (k_j r_j)^2}{r_j^2} v_{j,m} - \frac{2m}{r_j^2} u_{j,m} \right], \quad (9c)$$

$$-k_j p_{j,m} = \hat{\eta} \left[\frac{1}{r_j} \frac{\partial}{\partial r_j} \left[r_j \frac{\partial w_{j,m}}{\partial r_j} \right] - \frac{m^2 + (k_j r_j)^2}{r_j^2} w_{j,m} \right]. \quad (9d)$$

In (9), we omitted the superscripts c and d since these equations hold for both phases. The solution of (9) has already been discussed in [17]. Here, we only present the results. For $r < 1$ we find:

$$p_{j,m}^d(r_j, t) = 2\mu A_{j,m} I_m(k_j r_j), \quad m \geq 0, \quad (10a)$$

$$u_{j,0}^d(r_j, t) = A_{j,0} r_j I_0(k_j r_j) - \left[B_{j,0} + \frac{2}{k_j} A_{j,0} \right] I_1(k_j r_j), \quad (10b)$$

$$u_{j,m}^d(r_j, t) = A_{j,m}r_j I_m(k_j r_j) - \left[B_{j,m} + \frac{(m+2)}{k_j} A_{j,m} \right] I_{m+1}(k_j r_j) + \frac{C_{j,m}}{r_j} I_m(k_j r_j), \quad (11a)$$

$$v_{j,0}^d(r_j, t) = 0, \quad (11b)$$

$$v_{j,m}^d(r_j, t) = - \left[B_{j,m} + \frac{(m+2)}{k_j} A_{j,m} + \frac{k_j}{m} C_{j,m} \right] I_{m+1}(k_j r_j) - \frac{C_{j,m}}{r_j} I_m(k_j r_j), \quad (11c)$$

$$w_{j,m}^d(r_j, t) = -A_{j,m}r_j I_{m+1}(k_j r_j) + B_{j,m} I_m(k_j r_j), \quad m \geq 0, \quad (11d)$$

and for $r > 1$:

$$p_{j,m}^c(r, t) = 2D_{j,m}K_m(k_j r_j), \quad m \geq 0 \quad (12a)$$

$$u_{j,0}^c(r, t) = D_{j,0}r_j K_0(k_j r_j) + \left[E_{j,0} + \frac{2}{k_j} D_{j,0} \right] K_1(k_j r_j), \quad (12b)$$

$$u_{j,m}^c(r, t) = D_{j,m}r_j K_m(k_j r_j) + \left[E_{j,m} + \frac{(m+2)}{k_j} D_{j,m} \right] K_{m+1}(k_j r_j) + \frac{F_{j,m}}{r_j} K_m(k_j r_j), \quad (12c)$$

$$v_{j,0}^c(r, t) = 0, \quad (12d)$$

$$v_{j,m}^c(r, t) = \left[E_{j,m} + \frac{(m+2)}{k_j} D_{j,m} + \frac{k_j}{m} F_{j,m} \right] K_{m+1}(k_j r_j) - \frac{F_{j,m}}{r_j} K_m(k_j r_j), \quad (12e)$$

$$w_{j,m}^c(r, t) = D_{j,m}r_j K_{m+1}(k_j r_j) + E_{j,m} K_m(k_j r_j), \quad m \geq 0. \quad (12f)$$

Coefficients $A_{j,m}$, $B_{j,m}$, etc., depend on time t and are to be determined from the boundary conditions at the interface.

The solution for the continuous phase is influenced by all threads. As an *ansatz*, we represent the solution outside the threads by the linear combination of expansions like the one in (8) with respect to all the different threads; $j = 1, \dots, L$. This linear combination automatically satisfies the governing equations (4). Its coefficients will follow from the application of the boundary conditions around each thread. The addition of the velocities (u_j, v_j, w_j) is done vectorially, while the scalar quantities p_j are simply added. The resulting sums could be represented in any of the cylindrical coordinate systems of the L -threads. Taking for this

thread J and indicating this with subscript (J), we obtain the representations

$$p_{(J)}^c = \sum_{j=1}^L p_j^c, \quad (13a)$$

$$u_{(J)}^c = \sum_{j=1}^L \left[u_j^c \cos(\phi_J - \phi_j) + v_j^c \sin(\phi_J - \phi_j) \right], \quad (13b)$$

$$v_{(J)}^c = \sum_{j=1}^L \left[-u_j^c \sin(\phi_J - \phi_j) + v_j^c \cos(\phi_J - \phi_j) \right], \quad (13c)$$

$$w_{(J)}^c = \sum_{j=1}^L w_j^c. \quad (13d)$$

Let us consider the boundary conditions at the interface of thread J . Here, we apply a linearization procedure, *i.e.*, we evaluate the boundary conditions at the unperturbed thread ($R = 1$) and we only consider terms up to the first order in ϵ . The continuity of the velocities is written as

$$[[u]]_J = 0, \quad [[v]]_J = 0, \quad [[w]]_J = 0. \quad (14)$$

Here, $[[u]]_J \equiv u_J^d - u_{(J)}^c$ denotes the jump in the radial velocity at thread J . The other boundary conditions are the kinematic and the dynamic conditions. The kinematic boundary condition requires that

$$u_J^d = \frac{\partial R_J}{\partial t}. \quad (15)$$

The dynamic boundary conditions require that

$$[[\mathbf{n} \cdot \boldsymbol{\pi} \cdot \mathbf{t}]]_J = 0, \quad (16a)$$

$$[[\mathbf{n} \cdot \boldsymbol{\pi} \cdot \mathbf{n}]]_J = -\sigma \left(\frac{1}{R_1} + \frac{1}{R_2} \right). \quad (16b)$$

Here, \mathbf{n} is the unit normal vector pointing outwards, \mathbf{t} the unit tangent vector, σ the surface tension, R_1 and R_2 the principle radii of curvature, and $\boldsymbol{\pi}$ the total stress tensor defined by

$$\boldsymbol{\pi} = -p \boldsymbol{\delta} + \boldsymbol{\tau}, \quad (17a)$$

$$\boldsymbol{\tau} = \hat{\eta}[\nabla \mathbf{v} + (\nabla \mathbf{v})^T]. \quad (17b)$$

Here $\boldsymbol{\delta}$ is the unit tensor, $\boldsymbol{\tau}$ is the extra stress tensor, and T stands for the transpose. At thread J , the boundary conditions are, to first order,

$$[[\tau_{r\phi}]]_J = 0, \quad (18a)$$

$$[[\tau_{rz}]]_J = 0, \quad (18b)$$

$$[[-p + \tau_{rr}]]_J = - \left(\sum_{m=0}^{\infty} [m^2 + k^2 - 1] \varepsilon_{J,m}(t) \cos m\phi_J \right) \cos(k_J z - \alpha_J). \quad (18c)$$

In view of (11–13), the evaluation of the boundary conditions at thread J requires to expand the product of a Bessel function and a Fourier expansion with respect to thread j , $j \neq J$, around thread J . To handle this, we use the geometrical relations (2) and Graf's addition theorem of Bessel function (see [21, Formula 11.3(8)]). We finally obtain solutions by applying the method of moments.

2.1.2. Evaluation of boundary conditions

For clarity, we restrict ourselves in this section to the zero-order Fourier expansion, since this lowest mode already yields a reliable solution as shown in [17].

Let thread J , $1 \leq J \leq L$, be taken as frame of reference. The evaluation of boundary conditions at its interface requires to express all quantities in terms of (r_j, ϕ_j) . As an example, we will describe this for the continuity of the radial velocity. Since only phase differences are relevant, we may take $\alpha_J = 0$. Requiring $[[u]]_J = u_J^d - u_{(J)}^c = 0$ and using (7), (8), and (11–13), we obtain the condition:

$$X(t) \cos(k_J z) - \sum_{j \neq J} [Y(r_j, \phi_j, \phi_j, t)] \cos(k_j z - \alpha_j) = 0. \quad (19)$$

In general, X and Y are given by long expressions which provide little information. They will be made explicit below for $L = 3$. Here, the important point is that neither X and Y depends on z . Since (19) must be satisfied for all $z \in \mathbb{R}$, we conclude that the wave numbers k_J and k_j must be the same, so $k_j = k$ for all j . Moreover, the phases α_j take the values 0 or π . If $\alpha_j = 0$, thread j is in-phase with thread J , whereas for $\alpha_j = \pi$ thread j is out-of-phase with thread J . We remark that varying the values of α_j leads to various, so-called, *phase pattern*. We code a pattern by the vector

$$\mathbf{s}_n = (s_{n,1}, s_{n,2}, \dots, s_{n,L})^T, \text{ with } s_{n,j} = \pm 1 \text{ for } \begin{cases} j = 1, \dots, L \\ n = 1, \dots, 2^L \end{cases}. \quad (20)$$

Since we have L positions which may take binary values the number of patterns is 2^L . However, because of symmetry, many patterns will have identical break-up behaviour. For a given phase pattern \mathbf{s}_n , (19) reduces to

$$X(t) - \sum_{j \neq J} s_{n,j} [Y(r_j, \phi_j, \phi_j, t)] = 0. \quad (21)$$

Here, Y is still written in terms of (r_j, ϕ_j, ϕ_j) , but we can rewrite the r_j and ϕ_j dependences in terms of ϕ_J only. After changing the order of summations, we obtain

$$X(t) - \sum_{m=-\infty}^{\infty} \left(\sum_{j \neq J} s_{n,j} \hat{Y}(t; |j - J|kb) \right) \cos m\phi_J = 0. \quad (22)$$

Here, \hat{Y} results from expressing Y in terms of r_J and ϕ_J . Note that \hat{Y} contains $|j - J|b$, the distance between thread J and j . Taking the zero-moment of (22), *i.e.*, integrating over ϕ_J , we obtain

$$X(t) - \sum_{j \neq J} s_{n,j} \hat{Y}(t; |j - J|kb) = 0. \quad (23)$$

For the zero-order Fourier approach, we remark that we have $L \times 4$ unknown coefficients (see (11) and (12) for $m = 0$).

To illustrate the theory, we apply it to a system of three threads in a row as shown in Figure 1. Here, thread $J = 1$ is taken as reference system. For the zero-order Fourier mode, the azimuthal velocity v_1^d inside the thread vanishes (see (7)). However, $v_{(1)}^c$ does not vanish in general, as follows from (13), but since $v_{(1)}^c$ is, after applying Graf's addition theorem, an odd function in ϕ_1 , its zero-moment is zero. The same holds for $\tau_{r_1\phi_1}$. Retaining in (7) the $m = 0$ mode only, we have for $j = 1, 2, 3$,

$$p_j^d(r_j, \phi_j, z, t) = p_{j,0}^d(r_j, t) \cos(kz - \alpha_j), \quad (24a)$$

$$u_j^d(r_j, \phi_j, z, t) = u_{j,0}^d(r_j, t) \cos(kz - \alpha_j), \quad (24b)$$

$$w_j^d(r_j, \phi_j, z, t) = w_{j,0}^d(r_j, t) \sin(kz - \alpha_j), \quad (24c)$$

while (13) reads in this case as

$$p_{(1)}^c = p_1^c + p_2^c + p_3^c, \quad (25a)$$

$$u_{(1)}^c = u_1^c + u_2^c \cos(\phi_1 - \phi_2) + u_3^c \cos(\phi_1 - \phi_3), \quad (25b)$$

$$w_{(1)}^c = w_1^c + w_2^c + w_3^c. \quad (25c)$$

The evaluation of boundary conditions at the interface S_1 requires expressing all quantities in terms of (r_1, ϕ_1) . As an example, we will work this out for the continuity of the radial velocity. From $[[u]]_1 = u_1^d - u_{(1)}^c = 0$, we obtain the condition

$$X(t) \cos(kz) - \sum_{j=2}^3 [Y(r_j, \phi_1, \phi_j, t)] \cos(kz - \alpha_j) = 0, \quad (26)$$

where

$$\begin{aligned} X(t) = & \left(I_0(k) - \frac{2}{k} I_1(k) \right) A_{1,0}(t) - I_1(k) B_{1,0}(t) \\ & - \left(K_0(k) + \frac{2}{k} K_1(k) \right) D_{1,0}(t) - K_1(k) E_{1,0}(t), \end{aligned} \quad (27)$$

and

$$Y(r_j, \phi_1, \phi_j, t) = \left[\left(r_j K_0(kr_j) + \frac{2}{k} K_1(kr_j) \right) D_{j,0}(t) + E_{j,0}(t) K_1(kr_j) \right] \cos(\phi_1 - \phi_j). \quad (28)$$

We recall that, for convenience, we have taken $\alpha_1 = 0$. As argued above with respect to (19), Equation (26) implies that α_2 and α_3 can only attain the values 0 and π . This leads to the following phase patterns:

1. $\alpha_1 = 0, \alpha_2 = 0$, and $\alpha_3 = 0$, coded by $\mathbf{s}_1 = (1, 1, 1)^T$; all neighbouring threads disintegrate in-phase.
2. $\alpha_1 = 0, \alpha_2 = \pi$, and $\alpha_3 = 0$, coded by $\mathbf{s}_2 = (1, -1, 1)^T$; all neighbouring threads disintegrate out-of-phase.

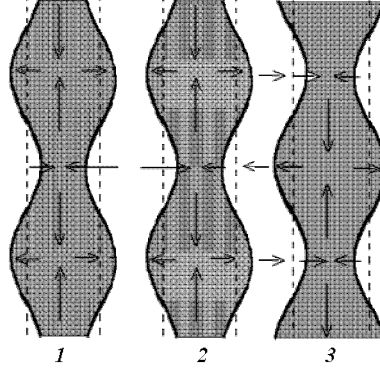


Figure 2. Top view of one of the possible phase patterns if $L = 3$. Thread 1 and 2 are in-phase and thread 2 and 3 are out-of-phase.

3. $\alpha_1 = 0, \alpha_2 = 0$, and $\alpha_3 = \pi$, coded by $\mathbf{s}_3 = (1, 1, -1)^T$; thread 3 disintegrates out-of-phase from thread 1 and 2.
4. $\alpha_1 = 0, \alpha_2 = \pi$, and $\alpha_3 = \pi$, coded by $\mathbf{s}_4 = (1, -1, -1)^T$; both threads 2 and 3 disintegrate out-of-phase from thread 1.

We remark that, in view of the symmetry of the system, cases 3 and 4 are identical. In Figure 2 one of the possible phase patterns for $L = 3$ is sketched. For given \mathbf{s}_n , condition (26) reduces to

$$X(t) - \sum_{j=2}^3 s_{n,j} [Y(r_j, \phi_1, \phi_j, t)] = 0. \quad (29)$$

Expressing all terms with respect to ϕ_1 and taking the zero-moment, we obtain

$$X(t) - \left(s_{n,2} \hat{Y}(t; kb) + s_{n,3} \hat{Y}(t; 2kb) \right) = 0. \quad (30)$$

The contribution of both thread 2 and 3 is given by the same expression \hat{Y} , but with different arguments kb and $2kb$. Evaluating the zero-moment of all boundary conditions and choosing an appropriate ordering of the unknowns, for a given \mathbf{s}_n ($n = 1, \dots, 8$), we arrive at a matrix equation for the unknown coefficients:

$$(\mathbf{H}\mathbf{D}_n)\mathbf{z}_n = \mathbf{D}_n\mathbf{e}, \quad (31)$$

where the matrices \mathbf{H} and \mathbf{D}_n are defined as

$$\mathbf{H} = \begin{pmatrix} \mathbf{H}_0 & \mathbf{H}_1 & \mathbf{H}_2 \\ \mathbf{H}_1 & \mathbf{H}_0 & \mathbf{H}_1 \\ \mathbf{H}_2 & \mathbf{H}_1 & \mathbf{H}_0 \end{pmatrix}, \quad \mathbf{D}_n = \begin{pmatrix} s_{n,1}\mathbf{I}_4 & \mathbf{0} & \mathbf{0} \\ \mathbf{0} & s_{n,2}\mathbf{I}_4 & \mathbf{0} \\ \mathbf{0} & \mathbf{0} & s_{n,3}\mathbf{I}_4 \end{pmatrix}, \quad (32)$$

with 4×4 submatrices \mathbf{H}_j and identity matrix \mathbf{I}_4 . The vectors \mathbf{z}_n and \mathbf{e} are given by $\mathbf{z}_n = (\mathbf{z}_{n,1}^T, \mathbf{z}_{n,2}^T, \mathbf{z}_{n,3}^T)^T$ and $\mathbf{e} = (\mathbf{e}_1^T, \mathbf{e}_2^T, \mathbf{e}_3^T)^T$ with

$$\mathbf{z}_{n,j}(t) = (A_{j,0}^{(n)}(t), B_{j,0}^{(n)}(t), D_{j,0}^{(n)}(t), E_{j,0}^{(n)}(t))^T \text{ and } \mathbf{e}_j = (0, 0, 0, (1 - k^2)\varepsilon_{j,0}(t))^T. \quad (33)$$

So, \mathbf{z}_n and \mathbf{e} have length 12. For convenience, we denote the components of \mathbf{z}_n by $z_{n,l}$. Explicit expressions for \mathbf{H}_j are given in Appendix A. The matrix \mathbf{H} depends on the numbering of the threads. However, this is just a matter of permutation. The solution of (31) is given by

$$z_{n,l} = (-1)^l s_{n,\lceil l/4 \rceil} \frac{1-k^2}{|\mathbf{H}|} \left(\sum_{j=1}^3 (s_{n,j} |\mathbf{H}_{(4j,l)}|) \varepsilon_{j,0}(t) \right), \quad (34)$$

where $\lceil x \rceil$ in $s_{n,\lceil x \rceil}$ is defined as the ceiling of x , *i.e.*, the smallest integer greater than or equal to x . Here, $|\cdot|$ denotes the determinant and $\mathbf{H}_{(4j,l)}$ is the 11×11 sub-matrix of \mathbf{H} which can be found by omitting the $(4j)$ -th row and the l -th column of \mathbf{H} . For example, we obtain

$$\begin{aligned} z_{n,1} &\equiv A_{1,0}^{(n)}(t) \\ &= -s_{n,1} \frac{1-k^2}{|\mathbf{H}|} (s_{n,1} |\mathbf{H}_{(4,1)}| \varepsilon_{1,0}(t) + s_{n,2} |\mathbf{H}_{(8,1)}| \varepsilon_{2,0}(t) + s_{n,3} |\mathbf{H}_{(12,1)}| \varepsilon_{3,0}(t)). \end{aligned} \quad (35)$$

We note that this coefficient is proportional to the amplitudes of the disturbances.

The extension from $L = 3$ to $L > 3$ is straightforward. For a given phase pattern \mathbf{s}_n , we then have $L \times 4$ unknown coefficients and

$$\mathbf{H} = \begin{pmatrix} \mathbf{H}_0 & \mathbf{H}_1 & \cdots & \mathbf{H}_{L-1} \\ \mathbf{H}_1 & \mathbf{H}_0 & \cdots & \mathbf{H}_{L-2} \\ \vdots & \vdots & & \vdots \\ \mathbf{H}_{L-1} & \mathbf{H}_{L-2} & \cdots & \mathbf{H}_0 \end{pmatrix}. \quad (36)$$

Equation (34) still holds with 3 replaced by L .

2.1.3. Stability analysis

To analyze the stability of the system we use the kinematic condition (15). For $j = 1, \dots, L$, and a given phase pattern \mathbf{s}_n ($n = 1, \dots, 2^L$) we obtain

$$\frac{d\varepsilon_{j,0}(t)}{dt} = u_{j,0}^d = \left(I_0(k) - \frac{2}{k} I_1(k) \right) A_{j,0}^{(n)}(t) - I_1(k) B_{j,0}^{(n)}(t), \quad (37)$$

where

$$\begin{aligned} A_{j,0}^{(n)}(t) &= z_{n,4j-3} = -s_{n,j} \frac{1-k^2}{|\mathbf{H}|} \left(\sum_{l=1}^L (s_{n,l} |\mathbf{H}_{(4l,4j-3)}|) \varepsilon_{l,0}(t) \right), \\ B_{j,0}^{(n)}(t) &= z_{n,4j-2} = s_{n,j} \frac{1-k^2}{|\mathbf{H}|} \left(\sum_{l=1}^L (s_{n,l} |\mathbf{H}_{(4l,4j-2)}|) \varepsilon_{l,0}(t) \right). \end{aligned} \quad (38)$$

Since $A_{j,0}^{(n)}(t)$ and $B_{j,0}^{(n)}(t)$ are linear combinations of the amplitudes, we may write

$$\frac{d}{dt}(s_{n,j} \varepsilon_{j,0}(t)) = \sum_{l=1}^L Q_{j,l} s_{n,l} \varepsilon_{l,0}(t), \quad (39)$$

with

$$Q_{j,l} = -\frac{1-k^2}{|\mathbf{H}|} \left([I_0(k) - \frac{2}{k}I_1(k)]|\mathbf{H}_{(4l,4j-3)}| + I_1(k)|\mathbf{H}_{(4l,4j-2)}| \right). \quad (40)$$

In (39), we have multiplied both sides of (37) by $s_{n,j}$. In matrix notation, we obtain

$$\frac{d\mathbf{E}}{dt} = \mathbf{Q}(b, \mu, k)\mathbf{E}, \quad (41)$$

where \mathbf{E} , with elements $s_{n,j}\varepsilon_{j,0}(t)$, is the vector of the disturbance amplitudes multiplied by the phase pattern component $s_{n,j}$, and \mathbf{Q} , with elements $Q_{j,l}$, is an L by L matrix depending on the distance b , the ratio of viscosities μ , and the wave number k . The stability of the L -threads system is determined by analyzing the structure of the solutions of (41). Since the dependence on phase pattern \mathbf{s}_n is now included in \mathbf{E} and the time dependence of any \mathbf{E} is determined by the eigenvalues of \mathbf{Q} , we may draw conclusions about the (in)stability of all phase patterns at the same time from only calculating the L eigenvalues q_j , $j = 1, \dots, L$. The eigenvectors \mathbf{x}_j of \mathbf{Q} play an important role. These eigenvectors form a basis for the space of possible initial perturbations $\mathbf{E}(0)$. It should be realized that each \mathbf{x}_j corresponds in a unique way to a phase pattern via the definition

$$\mathbf{s}_j = (\text{sign}(\mathbf{x}_j)_1, \text{sign}(\mathbf{x}_j)_2, \dots, \text{sign}(\mathbf{x}_j)_L)^T. \quad (42)$$

We call such a pattern \mathbf{s}_j a *basic phase pattern* and we have L of them. The time evolution of the j -th basic phase pattern is determined by the real part of q_j . Since a general phase pattern is a linear combination of the basic phase patterns, the (in)stability of the system follows from the (in)stability of the basic phase patterns, so from the q_j . The important conclusion is that, instead of optimizing over 2^L phase patterns, it suffices to calculate the L eigenvalues q_j of \mathbf{Q} . Per basic phase pattern we can calculate the growth rate $q_{j_{\max}}$ by optimizing the real part of q_j over all k . The growth rate q_{\max} of the system as a whole is then obtained by taking the maximum of the $q_{j_{\max}}$ over $j = 1, \dots, L$. As an illustration, for $L = 3$ results are given in Section 4.1.

2.2. TRIANGULAR AND ARBITRARY CONFIGURATIONS

Here, we show how the method presented above can easily be applied to more intricate configurations. For illustrative purposes we deal with the triangular configuration $\triangle O_1 O_2 O_3$ shown in Figure 3. Take the base line ℓ as the horizontal axis of the system, and let (r_i, ϕ_i, z) be cylindrical coordinates at thread i with ϕ_i measured counterclockwise with respect to ℓ , $b_{ij} = b_{ji}$ be the distance between threads i and j , and $\beta_{ij} = \beta_{ji}$ be the angle between the line b_{ij} and the axis ℓ . So, b_{12} coincides with the axis ℓ and $\beta_{12} = 0$. Scaling the radial direction r_i and the distance b_{ij} by a as in (6), and then omitting the stars notation in the sequel, we obtain the following geometrical relations for $j \neq J$ with $j, J = 1, 2, 3$:

$$r_J \cos \phi_J = r_j \cos \phi_j + \text{sgn}(j - J) \left(\sum_{l=l_m}^{J-1} b_{l,l+1} \cos \beta_{l,l+1} \right), \quad (43a)$$

$$r_J \sin \phi_J = r_j \sin \phi_j + \text{sgn}(j - J) \left(\sum_{l=l_m}^{J-1} b_{l,l+1} \sin \beta_{l,l+1} \right), \quad (43b)$$

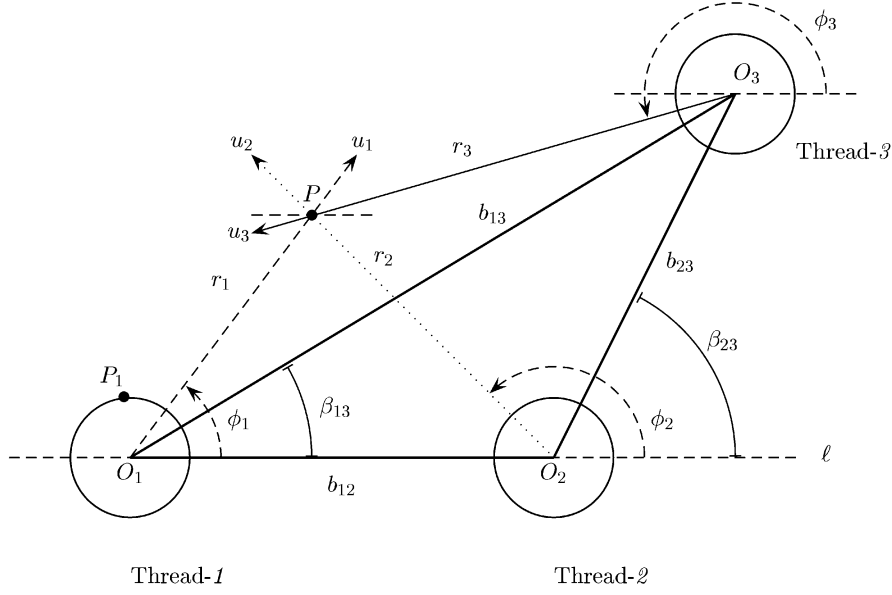


Figure 3. Coordinate system used for the triangular configuration. Extension to arbitrary configurations of L threads directly follows from this figure.

where $l_m = \min\{j, J\}$ and $l_M = \max\{j, J\}$, and $\text{sgn}(j - J)$ is the sign function defined as

$$\text{sgn}(j - J) = \begin{cases} -1, & j < J, \\ 0, & j = J, \\ 1, & j > J. \end{cases} \quad (44)$$

From Figure 3, we also obtain the relations:

$$r_J \cos(\phi_J - \beta_{Jj}) = r_j \cos(\phi_j - \beta_{Jj}) + \text{sgn}(j - J)b_{Jj}, \quad (45a)$$

$$r_J \sin(\phi_J - \beta_{Jj}) = r_j \sin(\phi_j - \beta_{Jj}). \quad (45b)$$

These relations are needed when evaluating the boundary conditions at the interfaces. The ideas for solving the creeping flow approximation are similar to those in previous section. Let us outline the method:

- Take (r_j, ϕ_j, z) as frame of reference and as general expressions for the solutions for the radial velocity, for $j \neq J$ with $j, J = 1, 2, 3$:

$$u_j(r_j, \phi_j, z, t) = \left(\sum_{m=0}^{\infty} u_{j,m}(r_j, t) \cos m(\phi_j - \beta_{Jj}) \right) \cos(k_j z - \alpha_j), \quad (46)$$

and analogous for v_j , w_j and p_j . As above, the solutions for the Fourier coefficients are given by (11) and (12).

- Next, take for the continuous phase of the whole system vector addition of the velocities and scalar addition of pressures. Evaluation of these additions leads to the forms written as in (13). The evaluation of boundary conditions leads to $k_j = k$ for all j 's and phase patterns. The evaluation also implies that the product of Bessel functions and a Fourier

expansion with respect to thread $j \neq J$, should be expressed as a product of functions with respect to thread J . To this end, we use Graf's addition theorem and the relations (43) and (45). To find a finite set of equations for the unknowns, we apply the method of moments and obtain (41). But now, the components of the matrix \mathbf{H} in (32) are \mathbf{H}_{ij} given in Appendix A and $\mathbf{H}_{00} \equiv \mathbf{H}_0$. From this point, the analysis is similar to the case of equally spaced threads in a row.

Results are shown in Section 4.2. For a system of L threads at random positions, the analysis directly follows from the triangular-thread system. The relations (13), (43) and (45) still hold. Again, there are 2^L phase patterns which are all essentially different if the configuration does not possess any symmetry. However, for the stability of the system one has to calculate only the stability of L basic phase patterns.

3. The special case of equal viscosities

If threads and surrounding fluid have equal viscosities, $\eta^d = \eta^c = \eta$, so $\mu = 1$, the stability of the system can be established nearly analytically. We shall work out the method in some detail for an arbitrary number threads in a row. Following the ideas of [20] for the one-thread system, we first focus on the jump S in the normal stress across the interface. For thread j , this jump is given by

$$S_j = \frac{\sigma}{a} \sum_{m=0}^{\infty} (1 - (k_j a)^2 - m^2) \varepsilon_{j,m}(t) \cos m\phi_j \cos(k_j z - \alpha_j), \quad (47)$$

where σ is the surface tension. The idea is to include the jump as a ring force in the momentum equation:

$$\nabla p_j = \eta \Delta \mathbf{v}_j + \mathbf{e}_r \delta(r_j - a) S_j. \quad (48)$$

Here, $\delta(r_j - a)$ is the delta function and \mathbf{e}_r is the unit vector in the radial direction. Using (6), (7) and the scaling:

$$S_j = \frac{\sigma}{a} S_j^*, \quad (49)$$

we obtain equations for the components of (48) and eventually arrive at an extension of (9):

$$0 = \frac{1}{r_j} \frac{\partial [r_j u_{j,m}]}{\partial r_j} + \frac{m}{r_j} v_{j,m} + k_j w_{j,m}, \quad (50a)$$

$$\begin{aligned} \frac{\partial p_{j,m}}{\partial r_j} &= \frac{1}{r_j} \frac{\partial}{\partial r_j} \left[r_j \frac{\partial u_{j,m}}{\partial r_j} \right] - \frac{m^2 + 1 + (k_j r_j)^2}{r_j^2} u_{j,m} - \frac{2m}{r_j^2} v_{j,m} \\ &\quad + \delta(r_j - 1)(1 - k_j^2 - m^2) \varepsilon_{j,m}, \end{aligned} \quad (50b)$$

$$-\frac{m}{r_j} p_{j,m} = \frac{1}{r_j} \frac{\partial}{\partial r_j} \left[r_j \frac{\partial v_{j,m}}{\partial r_j} \right] - \frac{m^2 + 1 + (k_j r_j)^2}{r_j^2} v_{j,m} - \frac{2m}{r_j^2} u_{j,m}, \quad (50c)$$

$$-k_j p_{j,m} = \frac{1}{r_j} \frac{\partial}{\partial r_j} \left[r_j \frac{\partial w_{j,m}}{\partial r_j} \right] - \frac{m^2 + (k_j r_j)^2}{r_j^2} w_{j,m}. \quad (50d)$$

Combining (50b) and (50c), we obtain

$$\begin{aligned} \frac{\partial p_{j,m}}{\partial r_j} - \frac{m}{r_j} p_{j,m} &= \left(\frac{1}{r_j} \frac{\partial}{\partial r_j} \left[r_j \frac{\partial}{\partial r_j} \right] - \frac{(m+1)^2 + (k_j r_j)^2}{r_j^2} \right) (u_{j,m} + v_{j,m}) \\ &\quad + \delta(r_j - 1)(1 - k_j^2 - m^2) \varepsilon_{j,m}, \end{aligned} \quad (51a)$$

$$\begin{aligned} \frac{\partial p_{j,m}}{\partial r_j} + \frac{m}{r_j} p_{j,m} &= \left(\frac{1}{r_j} \frac{\partial}{\partial r_j} \left[r_j \frac{\partial}{\partial r_j} \right] - \frac{(m-1)^2 + (k_j r_j)^2}{r_j^2} \right) (u_{j,m} - v_{j,m}) \\ &\quad + \delta(r_j - 1)(1 - k_j^2 - m^2) \varepsilon_{j,m}. \end{aligned} \quad (51b)$$

These equations, together with (50a) and (50d), can be solved by means of Hankel transforms. Let us denote these transforms and their inverses by

$$\begin{aligned} F_{j,n}^m(s) &\equiv \mathcal{H}_m\{f_{j,n}(r_j)\} = \int_0^\infty r_j J_m(sr_j) f_{j,n}(r_j) dr_j, \\ f_{j,n}(r_j) &\equiv \mathcal{H}_m^{-1}\{F_{j,n}^m(s)\} = \int_0^\infty s J_m(sr_j) F_{j,n}^m(s) ds. \end{aligned} \quad (52)$$

Here, J_m is the Bessel function of the first kind of order m . Applying the Hankel transforms, we obtain a system of linear equations in the variables $(U_{j,m}^{m+1} + V_{j,m}^{m+1})$, $(U_{j,m}^{m-1} - V_{j,m}^{m-1})$, $W_{j,m}^m$ and $P_{j,m}^m$:

$$0 = \frac{s}{2} [(U_{j,m}^{m+1} + V_{j,m}^{m+1}) - (U_{j,m}^{m-1} - V_{j,m}^{m-1})] + k_j W_{j,m}^m, \quad (53a)$$

$$s P_{j,m}^m = (s^2 + k_j^2)(U_{j,m}^{m+1} + V_{j,m}^{m+1}) - (1 - k_j^2 - m^2) J_{m+1}(s) \varepsilon_{j,m}, \quad (53b)$$

$$-s P_{j,m}^m = (s^2 + k_j^2)(U_{j,m}^{m-1} - V_{j,m}^{m-1}) - (1 - k_j^2 - m^2) J_{m-1}(s) \varepsilon_{j,m}, \quad (53c)$$

$$k_j P_{j,m}^m = (s^2 + k_j^2) W_{j,m}^m. \quad (53d)$$

Solving these linear equations and taking the inverse Hankel transform, we find for the m -th mode of the radial and azimuthal velocities

$$\begin{aligned} u_{j,m} &= \frac{(1 - k_j^2 - m^2) \varepsilon_{j,m}}{4} \left[\int_0^\infty \frac{s^3 + 2k_j^2 s}{(s^2 + k_j^2)^2} \left(J_{m+1}(s) J_{m+1}(sr_j) + J_{m-1}(s) J_{m-1}(sr_j) \right) ds \right. \\ &\quad \left. + \int_0^\infty \frac{s^3}{(s^2 + k_j^2)^2} \left(J_{m-1}(s) J_{m+1}(sr_j) + J_{m+1}(s) J_{m-1}(sr_j) \right) ds \right], \end{aligned} \quad (54a)$$

$$\begin{aligned} v_{j,m} &= \frac{(1 - k_j^2 - m^2) \varepsilon_{j,m}}{4} \left[\int_0^\infty \frac{s^3 + 2k_j^2 s}{(s^2 + k_j^2)^2} \left(J_{m+1}(s) J_{m+1}(sr_j) - J_{m-1}(s) J_{m-1}(sr_j) \right) ds \right. \\ &\quad \left. + \int_0^\infty \frac{s^3}{(s^2 + k_j^2)^2} \left(J_{m-1}(s) J_{m+1}(sr_j) - J_{m+1}(s) J_{m-1}(sr_j) \right) ds \right]. \end{aligned} \quad (54b)$$

Application of [21, Formula 13.53(6)] (an example of these evaluations is given in Appendix C) leads to

$$\begin{aligned}
u_{j,m} = & \frac{(1 - k_j^2 - m^2)}{4} \varepsilon_{j,m} \left[\frac{1}{2k_j} \frac{d}{dk_j} \left[k_j^2 \left(I_{m+1}(k_j) K_{m+1}(k_j r_j) + I_{m-1}(k_j) K_{m-1}(k_j r_j) \right) \right] \right. \\
& - k_j \frac{d}{dk_j} \left[I_{m+1}(k_j) K_{m+1}(k_j r_j) + I_{m-1}(k_j) K_{m-1}(k_j r_j) \right] \\
& \left. - \frac{1}{2k_j} \frac{d}{dk_j} \left[k_j^2 \left(I_{m-1}(k_j) K_{m+1}(k_j r_j) + I_{m+1}(k_j) K_{m-1}(k_j r_j) \right) \right] \right], \quad (55a)
\end{aligned}$$

$$\begin{aligned}
v_{j,m} = & \frac{(1 - k_j^2 - m^2)}{4} \varepsilon_{j,m} \left[\frac{1}{2k_j} \frac{d}{dk_j} \left[k_j^2 \left(I_{m+1}(k_j) K_{m+1}(k_j r_j) - I_{m-1}(k_j) K_{m-1}(k_j r_j) \right) \right] \right. \\
& - k_j \frac{d}{dk_j} \left[I_{m+1}(k_j) K_{m+1}(k_j r_j) - I_{m-1}(k_j) K_{m-1}(k_j r_j) \right] \\
& \left. - \frac{1}{2k_j} \frac{d}{dk_j} \left[k_j^2 \left(I_{m-1}(k_j) K_{m+1}(k_j r_j) - I_{m+1}(k_j) K_{m-1}(k_j r_j) \right) \right] \right]. \quad (55b)
\end{aligned}$$

Here, I_m and K_m are the modified Bessel functions. As a check on these intermediate results, we consider the $m = 0$ mode. The result is the zero-order Fourier mode of the radial velocity, given by

$$u_j(r_j, z) = k_j^2 (1 - k_j^2) \left(\int_0^\infty \frac{s J_1(s) J_1(sr_j)}{(s^2 + k_j^2)^2} ds \right) \varepsilon_{j,0}(t) \cos(k_j z - \alpha_j). \quad (56)$$

Rescaling to the full dimensions and taking $\alpha_j = 0$, we find that (56) is in agreement with the work of [20] for the axisymmetric break-up of a single liquid thread.

Next, consider L threads in a row, equally spaced with distances b . We shall restrict the discussion to the zero-mode solution, which implies $v_j = 0$. The radial velocity for the whole system is represented by (13b), with thread J as frame of reference. Hereafter, we omit the superscript c in (13b) since the fluids have equal viscosities. At the interface of thread J , substitution of (55a) for $m = 0$ in (13b) and application of Graf's addition theorem yield

$$u_{(J)} = A_{0,0}(k_J) \varepsilon_J(t) \cos k_J z + \sum_{j \neq J} \left(\sum_{n=-\infty}^{\infty} A_{n,j-J}(k_j, b) \cos n \phi_J \right) \varepsilon_{j,0}(t) \cos(k_j z - \alpha_j), \quad (57)$$

where

$$A_{0,0}(k_J) = -\frac{k_J(1 - k_J^2)}{2} \frac{d}{dk_J} \left[I_1(k_J) K_1(k_J) \right], \quad (58)$$

and

$$A_{n,j-J}(k_j, b) = \frac{k_j(1 - k_j^2)}{2} \frac{d}{dk} \left[I_1(k_j) K_n(|j - J|k_j b) I_{n-1}(k_J) \right]. \quad (59)$$

Note that $A_{n,j-J} = A_{n,J-j}$. On the other hand, according to (3) the interface velocity is given by

$$u_{(J)} = \dot{\varepsilon}_{J,0}(t) \cos k_J z. \quad (60)$$

Here, the overdot represents the derivative with respect to time t . Combining (57) and (60), we obtain

$$(A_{0,0}(k_j)\varepsilon_{J,0}(t) - \dot{\varepsilon}_{J,0}(t)) \cos k_J z + \sum_{j \neq J} \left(\sum_{n=-\infty}^{\infty} A_{n,j-J}(k_j, b) \cos n\phi_J \right) \varepsilon_{j,0}(t) \cos(k_j z - \alpha_j) = 0. \quad (61)$$

Condition (61) is only satisfied for all z if $k_j = k$ for all j . Moreover, α_j only takes the values 0 or π . Integration of (61) over the interval $[0, 2\pi]$ leads to

$$\dot{\varepsilon}_{J,0}(t) = A_{0,0}(k)\varepsilon_{J,0}(t) + \sum_{j \neq J} s_{n,j} A_{0,j-J}(k, b) \varepsilon_{j,0}(t), \quad (62)$$

with $s_{n,j}$ defined as in (20). Since we chose $s_{n,J} = 1$, we rewrite (62) as

$$s_{n,J} \dot{\varepsilon}_{J,0}(t) = \sum_{j=1}^L s_{n,j} A_{j-J} \varepsilon_{j,0}(t), \quad \text{with } A_{j-J} \equiv A_{0,j-J}. \quad (63)$$

Combination of all equations leads to a system of equations as in (41) where

$$\mathbf{Q} = \begin{pmatrix} A_0 & A_1 & A_2 & \cdots & A_{L-2} & A_{L-1} \\ A_1 & A_0 & A_1 & \cdots & \cdots & A_{L-2} \\ \vdots & \vdots & \vdots & \vdots & \vdots & \vdots \\ \vdots & \vdots & \vdots & \vdots & \vdots & \vdots \\ A_{L-2} & \cdots & \cdots & A_1 & A_0 & A_1 \\ A_{L-1} & A_{L-2} & \cdots & A_2 & A_1 & A_0 \end{pmatrix} \quad \text{and } \mathbf{E} \equiv \begin{pmatrix} s_{n,1} \varepsilon_{1,0}(t) \\ s_{n,2} \varepsilon_{2,0}(t) \\ \vdots \\ s_{n,L} \varepsilon_{L,0}(t) \end{pmatrix}. \quad (64)$$

The stability of the system is determined by the eigenvalues of \mathbf{Q} . For $L = 2$, the eigenvalues are simply given by

$$q^+ = A_0 + A_1, \quad \text{and } q^- = A_0 - A_1, \quad (65)$$

with eigenvectors $\mathbf{x}^+ = (1, 1)$ and $\mathbf{x}^- = (1, -1)$, respectively. The $q^+(q^-)$ are the growth rates of in-phase (out-of-phase) perturbations. Evaluating A_0 and A_1 , we obtain

$$q^\pm(k, b) = (1 - k^2) \left[I_1(k) K_1(k) + \frac{k}{2} \left(I_1(k) K_0(k) - I_0(k) K_1(k) \right) \pm I_1(k) \left([k I_0(k) - I_1(k)] K_0(kb) - \frac{kb}{2} I_1(k) K_1(kb) \right) \right]. \quad (66)$$

These results are in perfect agreement with [17] where we calculated this result directly from (41). If $b \rightarrow \infty$, when the system approaches the single thread case, the second term of

(66) vanishes and we arrive at the result of [20]. To determine the stability of the two-threads system, we can easily calculate the growth rate q_{\max} by optimizing over k .

For L large enough, we can find an upper bound for q_{\max} . In view of the Toeplitz form of matrix (64), we may exploit the following property (see [22]). Let the 2π -periodic function $h(\theta)$ be given by

$$h(\theta) = A_0 + 2 \sum_{n=1}^{L-1} A_n \cos n\theta, \quad (67)$$

then the eigenvalues of \mathbf{Q} in (64) are contained in the interval $[M_1, M_2]$ where $M_1 = \min_{0 \leq \theta \leq 2\pi} h(\theta)$, $M_2 = \max_{0 \leq \theta \leq 2\pi} h(\theta)$. Since $h(\theta)$ is bounded from above by

$$h(\theta) < |A_0| + 2 \sum_{n=1}^{L-1} |A_n|, \quad (68)$$

we may take

$$\bar{q}(a, k, b) = |A_0| + 2 \sum_{n=1}^{L-1} |A_n| \quad (69)$$

as an upper bound. As an illustration, results are given in Section 4.3 for $L = 2, 3$ and 10 threads.

4. Results

4.1. ROW CONFIGURATION

We apply the theory in Section 2.1 for $L = 3$; this illustrates the general cases satisfactorily. Fixing the geometrical parameter b and the material parameter μ , we calculate the eigenvalues q_j and eigenvectors \mathbf{x}_j of \mathbf{Q} defined by (40) and (41). We find that the eigenvectors $\mathbf{x}_1, \mathbf{x}_2$ and \mathbf{x}_3 give rise, via (42), to the basic phase patterns $(1, 1, 1)^T$, $(1, -1, 1)^T$ and $(1, 1, -1)^T$, respectively. In view of symmetry, the pattern $(1, -1, -1)^T$ has the same behaviour as $(1, 1, -1)^T$. We calculate the growth rates $q_{1\max}$, $q_{2\max}$ and $q_{3\max}$ by optimizing the eigenvalues q_1, q_2 and q_3 over all wave numbers k . In Figures 4 and 5 we have plotted $q_{1\max}$, $q_{2\max}$ and $q_{3\max}$ as functions of b , for two values of μ . The case $\mu = 0.04$ corresponds to a situation in which the threads are less viscous than the surrounding fluid, whereas for $\mu = 4$ it is the other way around. The growth rate q_{\max} of the system as a whole is determined by the envelope of the three curves. The figure provides the information in which pattern the break-up will occur. The figures show that this strongly depends on μ and b . For $\mu = 0.04$, $q_{2\max}$ is dominant for all b (see Figure 4). This implies that the threads will disintegrate out-of-phase. However, for $\mu = 4$, the curves cross at two critical distances $b_{cr,1}$ and $b_{cr,2}$ (see Figure 5b). If $b < b_{cr,1}$ the threads will break up in $(1, 1, 1)^T$ (in-phase pattern). If $b_{cr,1} < b < b_{cr,2}$ the threads will break up in the $(1, 1, -1)^T$ (mixed pattern), whereas for $b > b_{cr,2}$ the threads will break up $(1, -1, 1)^T$ (out-of-phase pattern).

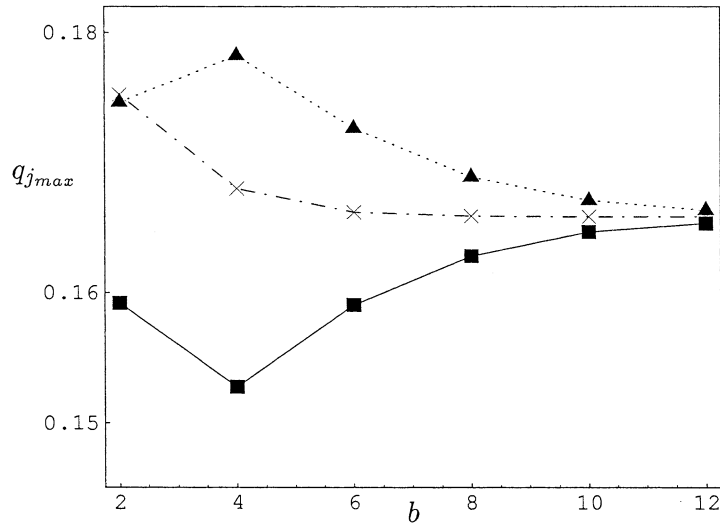


Figure 4. Curves of $q_{j_{\max}}$ as functions of b for $\mu = 0.04$. The patterns corresponding to $j = 1, 2$ and 3 are denoted by box, triangle and cross symbols, respectively.

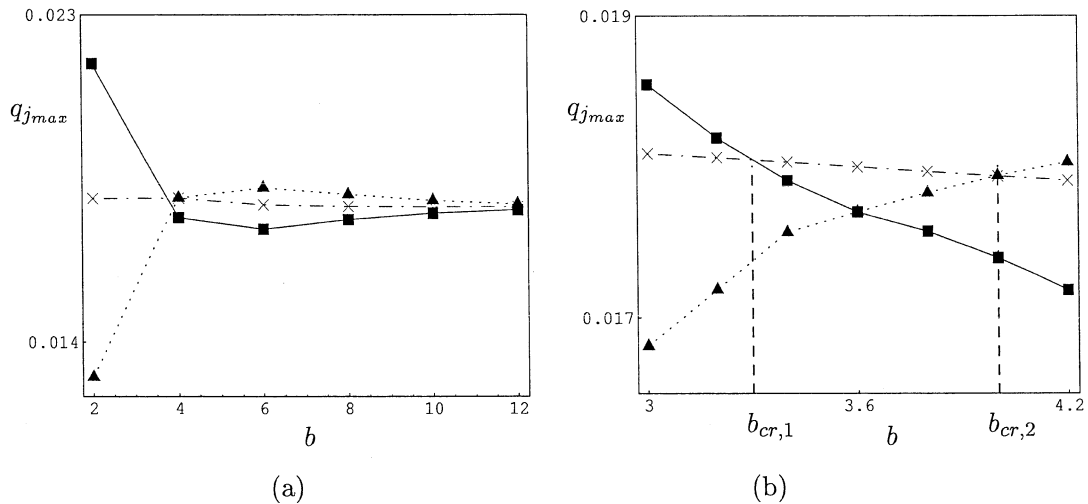


Figure 5. Same information as in Figure 4, but now for $\mu = 4$. Part (b) shows the details of the plot in the vicinity of the critical distances.

4.2. TRIANGULAR CONFIGURATION

First, we consider three threads at the vertices of an equilateral triangle. So, we take in Figure 3 $b_{12} = b_{23} = b$ and $\beta_{23} = 2\pi/3$. Fixing b and μ we calculate the eigensystem $\{q_j, \mathbf{x}_j\}$ of \mathbf{Q} . The growth rates $q_{j_{\max}} = \max_k \{q_j(b; \mu)\}$ as functions of b are shown in Figure 6 for two values of μ . In view of the symmetry of the system, we see that the growth rate $q_{2_{\max}}$ for the pattern $(1, -1, 1)^T$ coincides with $q_{3_{\max}}$ for the pattern $(1, 1, -1)^T$. Since the system has a lot of symmetry, it can break up in two patterns only. In the in-phase pattern all threads break up with the same phase, whereas out-of-phase break-up occurs if one thread has a phase

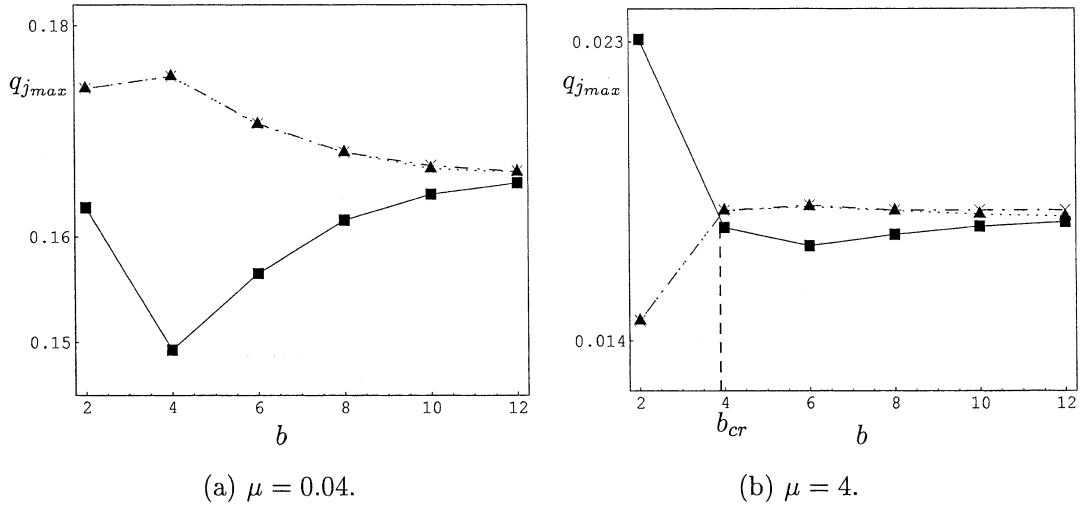


Figure 6. Same information as in Figure 4, but now for the equilateral triangle configuration.

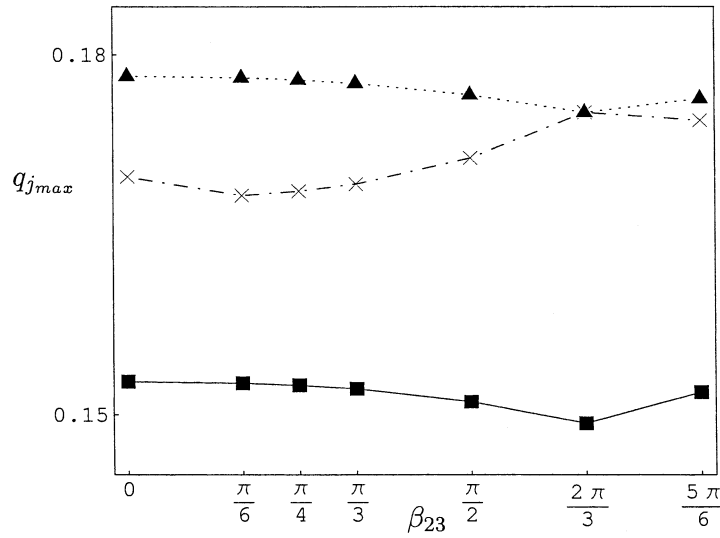


Figure 7. Curves of $q_{j_{max}}$ as functions of β_{23} for $\mu = 0.04$ and $b_{12} = b_{23} = 4$. The patterns corresponding to $j = 1, 2$ and 3 are denoted by box, triangle and cross symbols, respectively.

difference with the other two. For $\mu = 0.04$ we find that the system will break up out-of-phase for all b . For $\mu = 4$, we find a critical distance b_{cr} such that the system will break up either in-phase or out-of-phase.

We also calculate $q_{j_{max}}$ for non-equilateral triangle configurations by varying the angle β_{23} . In Figures 7 and 8 we plot $q_{j_{max}}$ as functions of β_{23} for two values of μ . For $\mu = 0.04$ and $b_{12} = b_{23} = 4$ we see that the $(1, -1, 1)^T$ pattern is dominant for all values of β_{23} (see Figure 7). For $\mu = 4$, in Figure 8a we find that $\beta_{23} = 2\pi/3$ is a critical angle such that for $\beta_{23} < 2\pi/3$ the $(1, 1, -1)^T$ is dominant and for $2\pi/3 < \beta_{23} < \pi$ the $(1, -1, 1)^T$. This depends on the value of b , e.g. for $\mu = 4$ and $b_{12} = b_{23} = 3$ the pattern $(1, 1, 1)^T$ is always dominant as shown in Figure 8b. In Figures 7 and 8 we see that the growth rates of the

patterns $(1, -1, 1)^T$ and $(1, 1, -1)^T$ are the same for $\beta_{23} = 2\pi/3$ since then the system has more symmetry.

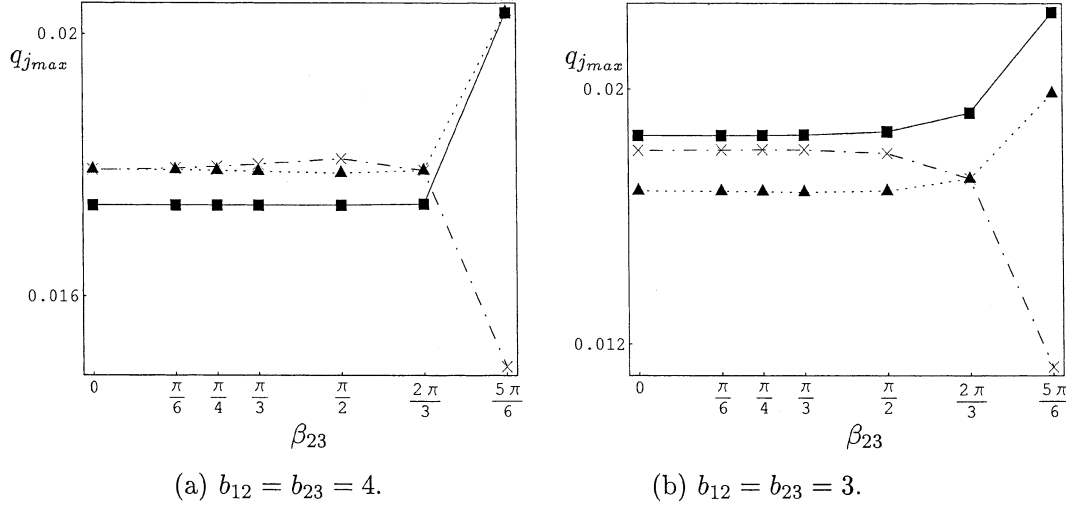


Figure 8. Same information as in Figure 7, but now for $\mu = 4$, and for two values of the sides length.

4.3. NO-VISCOSITY DIFFERENCES

For convenience, we define for the 2-threads system $q_{\max}^{\pm} \equiv \max_k \{q^{\pm}(k; b)\}$. These functions of b are shown in Figure 9a. We see that there exists a critical distance b_{cr} at which the dominant behaviour changes. As extra information we give in Figure 9b plots of $k_{\max}^+(b)$ and $k_{\max}^-(b)$, which are defined as those k values for which $q^+(k, b)$ and $q^-(k, b)$ attain their maximum values $q_{\max}^+(b)$ and $q_{\max}^-(b)$, respectively. The growth rate is given by the envelope of these curves, so by $q_{\max} = \max_k \{q^+(k; b), q^-(k; b)\}$ and shown in Figure 10 for $L = 2, 3$ and 10. We also calculate an estimate for \bar{q}_{\max} . Using a similar procedure for q_{\max} we obtain the results shown in Figure 11 for $L = 2$ and 10. Comparing the results \bar{q}_{\max} and q_{\max} , we see that this upper bound is quite a good approximation for the maximum growth rate, especially if $b \geq 3$.

5. General conclusions

In this paper, we have shown how the problem of the break-up of a cylindrical interface due to surface tension can be generalized to an arbitrary number of interacting immersed interfaces. By showing the principles of the theory for a row and a triangular configuration, we could explain how arbitrary numbers of threads in arbitrary configurations have to be treated. The two most general conclusions are as follows. First, all threads break up either in-phase or with a phase difference of π , *i.e.*, out-of-phase, with respect to the other threads. This implies that for a system with L threads, there are in principle 2^L phase patterns for break-up possible. However, since in practice any perturbation will tend to destabilize the system in a random fashion, the phase pattern with the highest growth rate will win and be observed. In this paper we have shown extensively how the growth rates of phase patterns can be calculated. In principle this would involve optimization over all possible phase patterns. Our second general

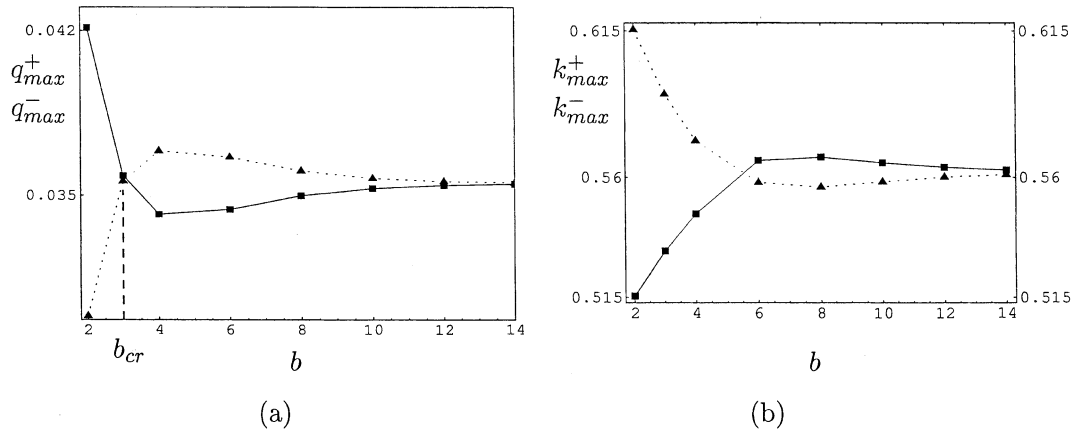


Figure 9. Curves of the growth rates q_{max}^+ (box) and q_{max}^- (triangle) and the corresponding wave number k_{max}^{\pm} as functions of b for the two-threads system.

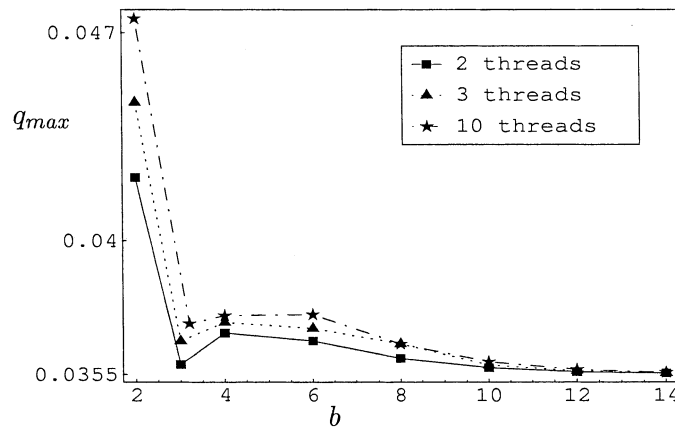


Figure 10. Curves of q_{max} as functions of b for systems with 2, 3 and 10 threads.

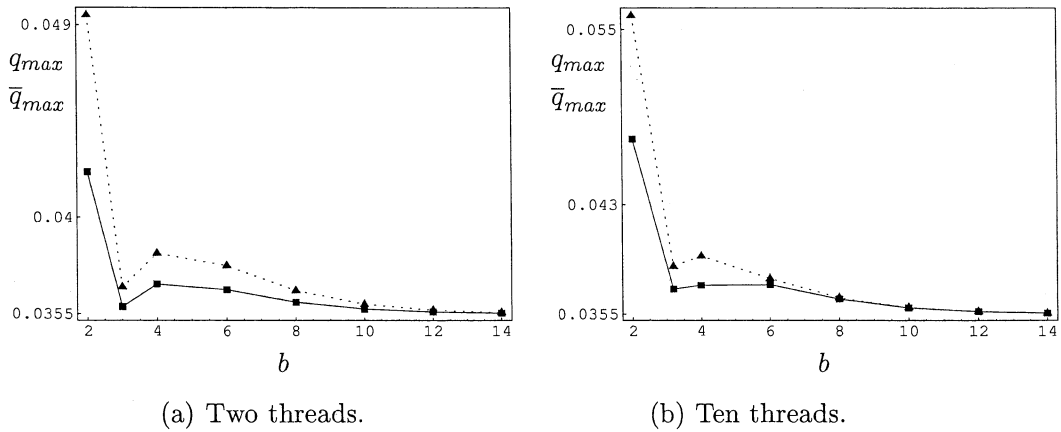


Figure 11. Comparison of calculated values of q_{max} (box) with the values of the upper bound \bar{q}_{max} (triangle) for two and ten threads.

conclusion is that this is not necessary, but that the optimization involves only the L so-called basic phase patterns. This reduces the amount of work considerably.

By applying the theory to specific cases we find that, in general, the ratio of viscosities of threads and solvent is a highly determining factor. If the threads are less viscous than the solvent, the break-up pattern with the threads out-of-phase is most unstable. If the threads are more viscous than the solvent, it is found that not one pattern is dominant. Then, it heavily depends on the details of the configuration which pattern will win. The system is found to exhibit a wealth of bifurcations: if a geometrical parameter is slightly varied, the system may suddenly change from one break-up pattern to another. For blending of viscous material this is important information, since out-of-phase patterns are more favourable for mixing than in-phase patterns.

We have also derived an analytical expression to estimate the growth rate for the special case of the fluids having equal viscosity. For L threads on a row we found an analytical upper bound, and showed via numerical simulations that this upper bound is quite close to the least upper bound.

Acknowledgements

This research is supported by QUE-Project (IBRD Loan No.4193-IND) of Departemen Matematika, Institut Teknologi Bandung, Indonesia.

Appendix A. Matrix \mathbf{H}

Explicit expressions for the block matrices \mathbf{H}_0 , \mathbf{H}_j and \mathbf{H}_{ij} , $i, j = 1, 2, \dots$.

$$\mathbf{H}_0 = \begin{pmatrix} kI_0(k) - 2I_1(k) & -kI_1(k) & -(kK_0(k) + 2K_1(k)) & -kK_1(k) \\ -kI_1(k) & kI_0(k) & -kK_1(k) & -kK_0(k) \\ -2\mu kI_1'(k) & 2\mu kI_1(k) & -2kK_1'(k) & 2kK_1(k) \\ 2\mu(kI_1(k) - 2I_1'(k)) & -2\mu kI_1'(k) & -2(2K_1'(k) - kK_1(k)) & -2kK_1'(k) \end{pmatrix}$$

$$\mathbf{H}_j = \begin{pmatrix} 0 & 0 & (jkbK_1(jkb)I_1(k) - kK_0(jkb)I_0(k) + 2K_0(jkb)I_1(k)) & kK_0(jkb)I_1(k) \\ 0 & 0 & -(jkbK_1(jkb)I_0(k) - kK_0(jkb)I_1(k)) & -kK_0(jkb)I_0(k) \\ 0 & 0 & -(2jkbK_1(jkb)I_1(k) - 2kK_0(jkb)I_0(k) + 2K_0(jkb)I_1(k)) & -2kK_0(jkb)I_1(k) \\ 0 & 0 & -2(kK_0(jkb)I_1(k) - jkbK_1(jkb)I_1'(k) - 2K_0(jkb)I_1'(k)) & 2kK_0(jkb)I_1'(k) \end{pmatrix}$$

$$\mathbf{H}_{ij} = \begin{pmatrix} 0 & 0 & (kb_{ij}K_1(kb_{ij})I_1(k) - kK_0(kb_{ij})I_0(k) + 2K_0(kb_{ij})I_1(k)) & kK_0(kb_{ij})I_1(k) \\ 0 & 0 & -(kb_{ij}K_1(kb_{ij})I_0(k) - kK_0(kb_{ij})I_1(k)) & -kK_0(kb_{ij})I_0(k) \\ 0 & 0 & -(2kb_{ij}K_1(kb_{ij})I_1(k) - 2kK_0(kb_{ij})I_0(k) + 2K_0(kb_{ij})I_1(k)) & -2kK_0(kb_{ij})I_1(k) \\ 0 & 0 & -2(kK_0(kb_{ij})I_1(k) - kb_{ij}K_1(kb_{ij})I_1'(k) - 2K_0(kb_{ij})I_1'(k)) & 2kK_0(kb_{ij})I_1'(k) \end{pmatrix}$$

Appendix B. Expressions derived from Graf's addition theorem

Let us consider Figure 3. As an illustration, we evaluate the product of Bessel function and a Fourier expansion of (r_3, ϕ_3) in terms of (r_1, ϕ_1) at point P_1 ($r_1 = 1$). For simplicity, take

$k_j = k$ for all j and introduce $\Phi_l = \phi_l - \beta_{13}$ for $l = 1, 3$. The addition theorem states that for $r_1 = 1 < b_{13}$,

$$\begin{aligned} K_m(kr_3) \cos m(\pi - \Phi_3) &= \sum_{n=-\infty}^{\infty} K_{m+n}(kb_{13}) I_n(k) \cos n\Phi_1 \\ &= (-1)^m K_m(kr_3) \cos m\Phi_3. \end{aligned} \quad (\text{B1})$$

The relation also holds with \cos replaced by \sin and $(-1)^m$ by $(-1)^{m+1}$. Using (45) and (B1) we find for $m \geq 0$,

$$\begin{aligned} r_3 K_m(kr_3) \cos m\Phi_3 \cos(\Phi_1 - \Phi_3) &= (-1)^m \sum_{n=-\infty}^{\infty} \left[K_{m+n}(kb_{13}) I_n(k) \right. \\ &\quad \left. - \frac{1}{2} b_{13} (K_{m+n-1}(kb_{13}) I_{n-1}(k) + K_{m+n+1}(kb_{13}) I_{n+1}(k)) \right] \cos n\Phi_1. \\ K_{m+1}(kr_3) \cos((m+1)\Phi_3 - \Phi_1) &= (-1)^{m+1} \sum_{n=-\infty}^{\infty} K_{m+n}(kb_{13}) I_{n-1}(k) \cos n\Phi_1. \\ K_{m-1}(kr_3) \cos((m-1)\Phi_3 + \Phi_1) &= (-1)^{m-1} \sum_{n=-\infty}^{\infty} K_{m+n}(kb_{13}) I_{n+1}(k) \cos n\Phi_1. \\ r_3 K_{m+1}(kr_3) \cos m\Phi_3 &= (-1)^{m+1} \sum_{n=-\infty}^{\infty} \left[K_{m+n}(kb_{13}) I_{n-1}(k) \right. \\ &\quad \left. - b_{13} K_{m+n+1}(kb_{13}) I_n(k) \right] \cos n\Phi_1. \end{aligned} \quad (\text{B2})$$

Appendix C. Evaluations of (54) and $A_{n,j-J}$

As for the evaluation of the expressions in (54), we only work out the $m = 0$ case, since the other cases follow analogously. From [21, Equation 13.53(6)], we have for n odd,

$$\cos\left(\frac{n+1}{2}\pi\right) \int_0^{\infty} \frac{s^n J_1(s) J_1(sr_j)}{s^2 + k_j^2} ds = -k_j^{n-1} I_1(k_j) K_1(k_j r_j), \quad (\text{C1})$$

provided that $r_j \geq 1$. Differentiating both sides of (C1) with respect to k_j , we obtain

$$\cos\left(\frac{n+1}{2}\pi\right) \int_0^{\infty} \frac{s^n J_1(s) J_1(sr_j)}{(s^2 + k_j^2)^2} ds = \frac{1}{2k_j} \frac{d}{dk_j} \left[k_j^{n-1} I_1(k_j) K_1(k_j r_j) \right]. \quad (\text{C2})$$

To calculate $A_{n,j-J}$, we proceed as follows:

$$\begin{aligned} u_{j,0} \cos(\phi_J - \phi_j) &= -\frac{k_j(1-k_j^2)}{2} \frac{d}{dk_j} \left[I_1(k_j) K_1(k_j r_j) \cos(\phi_J - \phi_j) \right] \\ &= \frac{k_j(1-k_j^2)}{2} \frac{d}{dk_j} \left[\sum_{n=-\infty}^{\infty} I_1(k_j) K_n(|j-J|k_j b) I_{n-1}(k_j r_j) \cos n\phi_J \right] \\ &= \sum_{n=-\infty}^{\infty} \left(\frac{k_j(1-k_j^2)}{2} \frac{d}{dk} \left[I_1(k_j) K_n(|j-J|k_j b) I_{n-1}(k_j r_j) \right] \right) \cos n\phi_J. \end{aligned} \quad (\text{C3})$$

Summation follows from the first formula of (B2). The interchange of the order of summation and differentiation is allowed thanks to the uniform convergence of the series. From (C3), since calculations are carried out at $r_j = 1$ we define

$$A_{n,j-J} = \frac{k_j(1 - k_j^2)}{2} \frac{d}{dk_j} \left[I_1(k_j) K_n(|j - J|kb) I_{n-1}(k_j) \right]. \quad (C4)$$

References

1. F. Savart, Memoire sur la Constitution des Veines liquides lancees par des orifices circulaires en mince paroi. *Annal. Chim. Phys.* 53 (1833) 337–374.
2. J. Plateau, Sur les figures d'Équilibre d'une masse liquide sans pesanteur. *Mémoires de l'Académie Royale de Belgique, nouvelle série* 23 (1849) 5.
3. L. Rayleigh, On the instability of jets. *Proc. London Math. Soc.* 10 (1878) 4–13.
4. L. Rayleigh, On the instability of a cylinder of viscous liquid under the capillary force. *Phil. Mag.* 34 (1892) 145–154.
5. S. Tomotika, On the instability of a cylindrical thread of a viscous liquid surrounded by another viscous fluid. *Proc. R. Soc. London A* 150 (1935) 322–337.
6. S. Tomotika, Breaking up of a drop of viscous liquid immersed in another viscous fluid which is extending at a uniform rate. *Proc. R. Soc. London A* 153 (1936) 302–318.
7. B.J. Meister and G.F. Scheele, Generalized solution of the Tomotika stability analysis for a cylindrical jet. *AIChE J.* 13 (1967) 682–688.
8. T. Mikami, R.G. Cox and S.G. Mason, Breakup of extending liquid threads. *Int. J. Multiphase Flow* 2 (1975) 113–138.
9. D.V. Khakhar and J.M. Ottino, Breakup of liquid threads in linear flows. *Int. J. Multiphase Flow* 13 (1987) 71–86.
10. K.O. Mikaelian, Effect of viscosity on Rayleigh-Taylor and Richtmyer-Meshkov instabilities. *Phys. Rev. E* 47 (1993) 375–383.
11. K.O. Mikaelian, Rayleigh-Taylor instability in finite-thickness fluids with viscosity and surface tension. *Phys. Rev. E* 54 (1996) 3676–3680.
12. J. Eggers, Universal pinching of 3D axisymmetric free-surface flow. *Phys. Rev. Lett.* 71 (1993) 3458–3460.
13. J. Eggers, Theory of drop formation. *Phys. Fluids* 7 (1995) 941–953.
14. C.M. Kinoshita, H. Teng and S.M. Masutani, A study of the instability of liquid jets and comparison with Tomotika's analysis. *Int. J. Multiphase Flow* 20 (1994) 523–533.
15. D.T. Papageorgiou, On the breakup of viscous liquid threads. *Phys. Fluids* 7 (1995) 1529–1544.
16. J. Eggers, Nonlinear dynamics and breakup of free surfaces flows. *Rev. Mod. Phys.* 3 (1997) 865–929.
17. A.Y. Gunawan, J. Molenaar and A.A.F. van de Ven, In-phase and out-of-phase break-up of two immersed liquid threads under influence of surface tension. *Eur. J. Mech. B/Fluids* 21 (2002) 399–412.
18. Y.M.M. Knops, *Morphology Development in Polymer Blends: The Hydrodynamic Interaction Between Disintegrating Threads*. Eindhoven: TU-Eindhoven (1997) 68pp.
19. Y.M.M. Knops, J.J.M. Slot, P.H.M. Elemans and M.J.H. Bulters, Simultaneous breakup of multiple viscous threads surrounded by viscous liquid. *AIChE J.* 47 (2001) 1740–1745.
20. H.A. Stone and M.P. Brenner, Note on the capillary thread instability for fluids of equal viscosities. *J. Fluid Mech.* 318 (1996) 373–374.
21. G.N. Watson, *A Treatise on the Theory of Bessel Functions*. Cambridge: University Press (1966) 804pp.
22. H. Widom, Toeplitz matrices. In: I.I. Hirschman, Jr. (ed), *MAA Studies in Mathematics. Vol. 3: Studies in Real and Complex Analysis*. New Jersey: Prentice-Hall, Inc. (1965) pp. 179–209.